

# Chapter 2

## Fabrication of Microfluidic Devices

M. Leester-Schädel, T. Lorenz, F. Jürgens, and C. Richter

**Abstract** Microfluidics could not be thought about without advances in micro- and nanofabrication. Following an approach that has been adapted from microelectronics fabrication is carried out in a cleanroom environment using monocrystalline silicon as base material. It typically involves mask-based photolithography, dry and wet etching and thin film deposition. Glass can be used as an alternative or in combination with silicon and allows optical access to the fluid in the microdevices. A different approach using the so-called soft lithography and PDMS (polydimethylsiloxane) material has found widespread applications because it is relatively cheap and easy to use. In most cases the manipulation of fluids at microscales takes place in closed volumes or channels. Several bonding techniques have been developed allowing closure by a lid which in many cases can be transparent. Recently, maskless techniques like inkjet- or 3D-printing, laser micromachining, and microelectrical discharge machining get more and more attention.

### 2.1 Introduction

Over the past several years there has been an increased interest in micromachining technologies. Today, microelectromechanical systems (MEMS), microoptoelectromechanical systems (MOEMS), and microfluidic systems can be found in nearly every manufacturing and industry segment (aerospace, medical appliance, automotive, communication technology, and safety engineering). Biotechnology and pharmaceutical process engineering are just joining the user group of mainly microfluidic systems. Innovative BioMEMS, Lab-on-Chip and Organ-on-Chip systems are being created.

The term “microsystem” has a variety of definitions. Usually, the sizes of functional microsystem parts are in the range of 10 nm and 100  $\mu\text{m}$ . Depending on the application, a complete microsystem has dimensions of up to some 10 mm.

---

M. Leester-Schädel (✉) • T. Lorenz • F. Jürgens • C. Richter  
IMT—Institute of Microtechnology, Technische Universität Braunschweig,  
Alte Salzdahlumer Str. 203, Braunschweig 38124, Germany  
e-mail: [m.leester@tu-braunschweig.de](mailto:m.leester@tu-braunschweig.de)

The fabrication of microsystems began in 1968 with semiconductor devices like diodes, transistors, integrated circuits, and later more complex electronic components. Especially communication and information technologies have profited significantly from these challenging advancements. Due to the excellent mechanical properties of silicon, which was and still is the most widely used semiconductor material, the semiconductor fabrication technologies have been further developed since the 1980s to build up 3D micromechanical systems. Today many different deposition, etching, second cast, bonding and as a newer achievement maskless patterning techniques are available to micromachine materials like polymers, silicon, glass, and metals. The key fabrication process is still the photolithography, based on a light-sensitive material (photoresist), in which the microstructures are transferred by exposing and developing.

Usually, the source material is a circular thin wafer with a diameter of 25 mm ( $\approx 1''$ ) to 300 mm ( $\approx 12''$ ). This wafer is machined as a whole (batch or wafer-level fabrication) as long as possible. The single microsystems are separated only in one of the last process steps. The main advantage of wafer-level micromachining is cost reduction for the single microsystem, because a few hundred devices can be fabricated at once, depending on the size of the micro device and the wafer. Industrial microfabrication is even specified for the simultaneous machining of up to 25 wafers.

## **2.2 Cleanroom**

A low-particle environment is essential to manufacture semiconductor components and microsystems, as well as pharmaceutical products, medical and life science devices. Therefore, it is essential to minimize the level of contamination by dust, airborne particles, aerosol particles, and chemical vapors, which leads to degradation of product performance on the one hand, and cross-infection between medical staff and patients in the healthcare industry on the other hand.

### **2.2.1 Classification**

A cleanroom is an environment with a controlled level of pollutants, temperature, humidity, and pressure. The contamination level of particulate matter is graded by the maximum allowable number of particles per unit volume (usually cubic meters) at a specified particle size. A discrete-particle-counting, light-scattering instrument is used to determine the concentration of airborne particles, equal to and larger than the specified sizes, at designated sampling spots [12]. Designation ISO 1 to ISO 9 refers to ISO 14644-1 standards, which specify the decimal logarithm of the number of particles with a size of  $0.1\text{ }\mu\text{m}$  or larger permitted per cubic meter of air. For example, the ambient air outside in a typical urban environment contains one

billion ( $10^9$ ) particles per cubic meter in the size range  $0.1\text{ }\mu\text{m}$  and larger in diameter, corresponding to an ISO 9 cleanroom. An ISO 5 cleanroom has at most  $10,000\text{ particles/m}^3$  and an ISO 1 cleanroom allows ten particles in that size range and no particles above  $0.2\text{ }\mu\text{m}$ . For pharmaceutical and biotechnological use, the number of maximum non-particulate contaminants such as microbes or germs must be monitored and limited according to the guidelines of good manufacturing practice [11].

To ensure a defined cleanroom class first the air entering from outside is filtered to exclude dust. Second the air inside is constantly recirculated through high-efficiency particulate air (HEPA) and/or ultra-low particulate air (ULPA) filters to remove internally generated contaminants. By applying either laminar air flow or turbulent air flow techniques to the environment air, any pollution is directed away from the workspace. Cleanroom architecture and equipment that promotes uncontrolled turbulence is to be avoided.

Personnel working in cleanrooms are another main particle source. To minimize the emission of contaminants naturally generated by skin, body, and garments the cleanroom staff has to wear special clothing (Fig. 2.1). The clothing itself is made of synthetics to be abrasion-resistant, lint-free, and impermeable to fibers and particles emitted of the undergarments. Furthermore, the cleanroom staff has to enter and exit the cleanroom through airlocks or air showers.

**Fig. 2.1** Cleanroom garments for ISO 5: (a) head cover, beard cover, coverall, overshoes, latex disposable gloves and (b) hairnet, coverall, shoes, nitrile disposable gloves



### 2.2.2 Cleanroom Concepts

There are different concepts to build up a cleanroom, which vary by size, acquisition costs, and modularity or rather modifiability. A complete room with individual size and design, which fulfills the requirements of the intended ISO class, is a cleanroom in the proper meaning of the word (conventional cleanroom). This is the largest but the most expensive and the fewest modifiable concept. Today, many different wall, ceiling, and floor systems are available. Their surfaces have to be easily cleanable, resistant against solvents and other chemicals and abrasion-free. In addition cleanroom systems have to fulfill high demands concerning lighting, vibration damping, electrostatic charge, and noise level. Changing rooms, airlock/air shower systems, integrated air guidance, and integrated media supply are also part of modern cleanroom systems. As an example, the cleanroom at the Institute of Microtechnology, TU Braunschweig, has 300 m<sup>2</sup> working space, divided into three ISO 5-6 corridors (Fig. 2.2). Behind and between these so-called white aisles are service (“gray”) aisles with a lower ISO class. This design has the advantage to get a large wall surface where process facilities and equipment can be integrated and installed.

A minienvironment (local cleanroom) is a high ISO class area within a lower ISO class laboratory. The high ISO class area is separated by PVC-strip or -film curtains and provided with filtered laminar airflow by an external laminar flow unit. The advantages are significant lower acquisition and operating costs, which are in contrast to the strongly limited space. A cleanroom cabin contains process facilities and working space as well as a laminar flow unit and can be integrated in laboratories or workshops without any complex external supply technology. This makes cleanroom cabins very flexible and consumer-adaptable. The most cost-saving and modifiable cleanroom concept is a tent, which is comparable to a cleanroom cabin but with PVC-film curtains instead of massive walls. This is the easiest way to realize a high ISO class in the direct surrounding of a process facility, for example a laser machine, but it cannot be used to install a fully equipped workplace with secure cleanroom conditions.



**Fig. 2.2** The three “white” cleanroom corridors in the Institute of Microtechnology at TU Braunschweig: (a) process unit aisle; (b) area of chemical processing and (c) yellow-light aisle for photolithography

### 2.2.3 Cleanroom Equipment

The above-mentioned properties are largely valid for semiconductor/microsystem as well as for pharmaceutical/biological/medical cleanrooms. The laminar flow in semiconductor/microsystem cleanrooms used for particle reduction requires the surfaces of workbenches, tables, etc. to be perforated. Polymers like melamine resin, polypropylene (PP), and polyvinylidene fluoride (PVDF) are popular materials for semiconductor cleanroom equipment. In contrast, the equipment surfaces of pharmaceutical cleanrooms have to be closed and sealed and are normally made of stainless steel as an easy-to-sterilize material.

## 2.3 Materials

### 2.3.1 Polydimethylsiloxane

In the field of microfluidics and microoptics polydimethylsiloxane (PDMS) has gained increasing interest in the last two decades. The main reasons are the fast, easy, and cost-effective fabrication process of PDMS using softlithography.

PDMS has a unique combination of properties resulting from the presence of an inorganic siloxane backbone and organic methyl groups attached to silicon [7]. Therefore it belongs to a group of polymeric organosilicon compounds that are commonly referred to as silicones [17]. The chemical formula for PDMS is  $\text{CH}_3[\text{Si}(\text{CH}_3)_2\text{O}]_n\text{Si}(\text{CH}_3)_3$ . PDMS provides a good chemical stability and is not hydroscopic. Furthermore, it is inert, nontoxic, biocompatible, nonflammable, optically transparent down to  $\lambda = 300$  nm and permeable to nonpolar gases like oxygen. PDMS is durable and has good thermal stability (up to 186 °C in air), a dielectric strength of 21 kV/mm and a dielectric constant of 2.7 stable over a wide frequency range [15], is isotropic and homogeneous, commercial available (e.g., Sylgard 184 by Dow Corning Inc.), and inexpensive [35]. It provides easy handling and can be bonded to itself and a series of other materials after oxygen or air plasma treatment [20]. However, there are some disadvantages accompanying these benefits: (a) PDMS shrinks by about 1 % upon curing; and the cured PDMS can be readily swelled by a number of nonpolar organic solvents such as toluene and hexane, (b) the elasticity and thermal expansion of PDMS may limit its utility in multilayer fabrication and/or nanofabrication, (c) its softness limits the aspect ratio of microstructures in PDMS, and (d) it can absorb drugs, proteins, and small hydrophobic molecules [33].

At room temperature PDMS is liquid and can be converted into solid elastomers by cross-linking. The polymerization is described by the example of the elastomer kit sylgard 184 from Dow Corning Inc.: The two components, siloxane oligomer and curing agent, are mixed in a mixing ratio depending on the intended Young's modulus of the elastomer (usually 10:1; if this ratio is increased, the Young's

**Fig. 2.3** Micro bioreactor made of PDMS. Further details about the system will be given in Sect. 5.4.2



modulus decreases). The polymerization proceeds by a hydrosilylation reaction, where the vinyl groups ( $\text{CH}_2=\text{CH}^-$ ) of the siloxane oligomers form covalent bonds with the hydrosilane ( $\text{SiH}$ ) groups of the curing agent. The cross-linking reaction is catalyzed by a platinum-catalyst contained in the curing agent and takes place at room temperature but can be accelerated by enhancing the temperature [19] (Fig. 2.3).

### 2.3.2 SU-8

SU-8 is a UV-sensitive, high-contrast, epoxy-based negative tone photoresist designed for the lithography of ultra-thick resists. It is ideally suited for imaging permanent microstructures with high-aspect ratios and near vertical sidewalls [24]. There are already many examples of its use as material for micromolds, packaging, and devices [18]. SU-8 is based on the epon SU-8 epoxy resin, which is a multifunctional glycidyl ether derivative of bisphenol-A novolac, providing an epoxy group functionality of 8 (hence the “8” in SU-8). The epoxy resin is dissolved in an organic solvent (cyclopentanone  $\text{C}_5\text{H}_8\text{O}$ ) with the addition of triarylsulfonium hexafluoroantimonate salt as photoinitiator. Depending on the quantity of solvent, SU-8 is available in different viscosities resulting in different layer thicknesses (e.g., SU-8 2005, SU-8 2025, and SU-8 2050 from MicroChem Corporation, which cover the thickness range from 1–2 to 250  $\mu\text{m}$  per layer). Higher thicknesses can be achieved in a multilayer process.

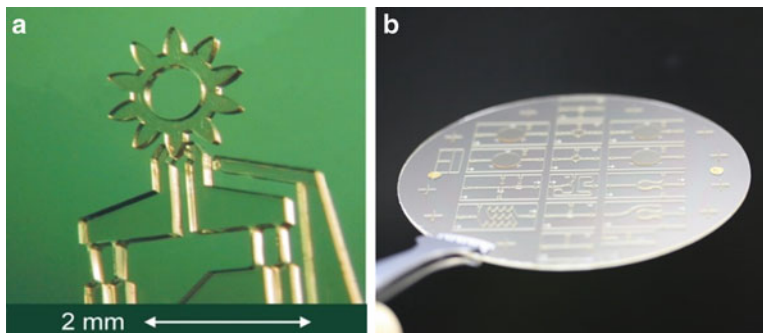


**Fig. 2.4** *Left:* Microgripper and microgear made of SU-8, *right:* fluidic SU-8 structures on a carrier wafer

The exposure at conventional near UV radiation (350–400 nm; i-line (365 nm) is recommended) transforms the triarylsulfonium hexafluoroantimonate salt into a photoacid ( $\text{H}^+ \text{SbF}_6^-$ ). The photoacid acts as a catalyst in the subsequent cross-linking reaction, whereby the  $\text{H}^+$  ions attack the cyclic bonds of the epoxy groups so that they open up and, as an avalanche effect, deliver another  $\text{H}^+$  ion. The open bonds cross-link to each other, so that the exposed areas become insoluble to liquid developers. The cross-linking process has to be enhanced by heat, requiring a post-exposure bake (PEB) at temperatures between 60 and 100 °C. The complete photolithography sequence is described in Sect. 2.5 (Fig. 2.4).

### 2.3.3 Silicon

The triumphal procession of single-crystalline silicon as substrate and polycrystalline silicon as thin film material has started in the semiconductor technology. Its excellent mechanical properties and the feasibility of integrating sensing and electronics on the same substrate have enabled the progression to MEMS. To fabricate functional silicon structures, many different techniques are available and well established. A distinction is made between surface micromachining, where the substrate stays unmachined and movable parts are fabricated by thin film deposition and subsequent removing of an underlying sacrificial layer, and bulk micromachining, where the microstructure is made by etching the substrate. The most popular etching techniques are described in Sect. 2.6.

Silicon is a semiconductor material, which means, that it is an insulator at low temperatures and a conductor at higher temperatures. Furthermore, the electrical conductivity can be enlarged, when foreign atoms (e.g., phosphor, brome) are added and integrated into the silicon lattice (doping [22]). However, for pure microfluidic components like channels, nozzles, and passive valves, mainly the mechanical properties of silicon and the suitability for etching and structuring are

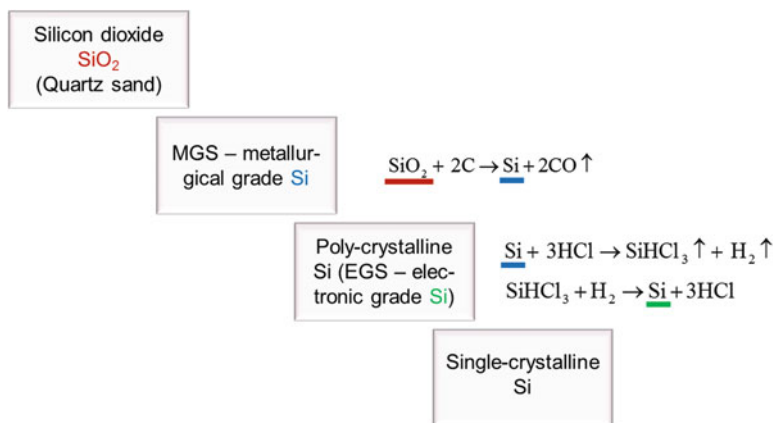


**Fig. 2.5** Fabrication steps of single-crystalline silicon

relevant. As well silicon is a favorite material for medical technologies and chemical engineering, because it is medical compatible and chemically stable. The semiconductor characteristics become important, when sensor functions shall be integrated into the microfluidic chip.

Single-crystalline silicon substrates are available as circular wafers of 25 mm ( $\approx 1''$ ) to 300 mm ( $\approx 12''$ ). They are polished either on one or on both sides, and can be doped differently. The fabrication of high-purity single-crystalline silicon consists of several steps (Fig. 2.5). The basic material is natural silicon dioxide  $\text{SiO}_2$  (quartz sand), which is reduced with carbon plus mild steel at a temperature of  $1400^\circ\text{C}$  to elemental metallurgical grade silicon (MGS) with a purity of 96–98 %. In the next step the MGS reacts with hydrochloric acid to trichlorosilane, which is then cooled down and slowly heated up again to remove most of the impurities. The back reaction to silicon takes place in a cold wall reactor with high-purity silicon cores. The result is polycrystalline electronic grade silicon (EGS) with a purity of 99.99999 %. The last step is the transformation to single-crystalline silicon in a Czochralski crystal growing furnace or by using float-zone pulling technology. Both methods base on a silicon seed crystal, which defines the crystal orientation. By pulling the seed crystal very slowly out of melted EGS, a single-crystalline silicon ingot arises (Czochralski method). With the float-zone pulling technology an EGS ingot is melted zonewise, beginning at the seed crystal. The latter method achieves the highest purity resulting in an electric resistivity of nearly  $2000\ \Omega\text{ cm}$ , but is more expensive than the Czochralski method ( $< 50\ \Omega\text{ cm}$ ). Afterwards the ingot is labeled with grinded flats and notches to indicate the crystal orientation and finally sawed into disks (wafers) with typical thicknesses of 50–5000  $\mu\text{m}$  [30].

The crystal structure of silicon is cubic face-centered (Fig. 2.6). Planes and directions are identified by Miller indices. To determine the Miller indices of a plane, one takes the intercept of that plane with the axes of an orthogonal coordinate system. Then, the reciprocal of the axis sections is taken and multiplied by the



**Fig. 2.6** Cubic face-centered crystal lattice (red dots) with primitive unit cell (green dots)

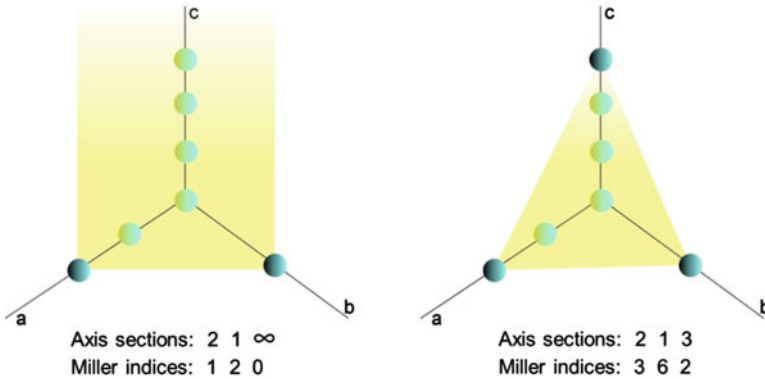
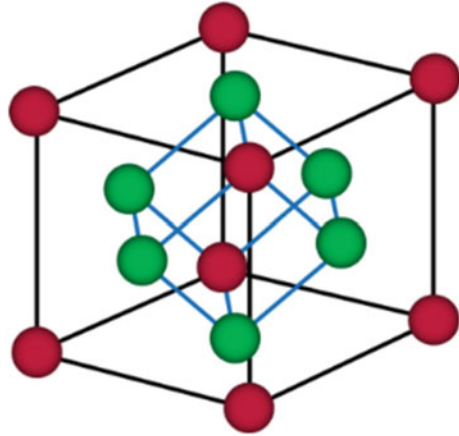


**Fig. 2.7** Examples of crystal planes—points of intersection with the crystal axes plus Miller indices

smallest common denominator. The ensuring numerators are the Miller indices ( $hkl$ ). Figure 2.7 shows two different crystal planes, their axis sections, and the related Miller indices.

Miller indices written in round brackets ( $hkl$ ) describe one specific plane. Equivalent planes are written with closed brackets  $\{hkl\}$ . One specific direction, which is perpendicular to the plane, is defined with angle brackets  $\langle hkl \rangle$ , equivalent directions with square brackets  $[hkl]$ . For a negative Miller index, the numeral is overlined ( $h\bar{k}\bar{l}$ ). Figure 2.8 shows exemplary the position of the (100), the (110), and the (111) silicon crystal plane.

The silicon crystal planes are characterized by remarkable differences to each other concerning their mechanical properties as well as their etch behavior in specific wet chemical etch solutions. For example, in potassium hydroxide

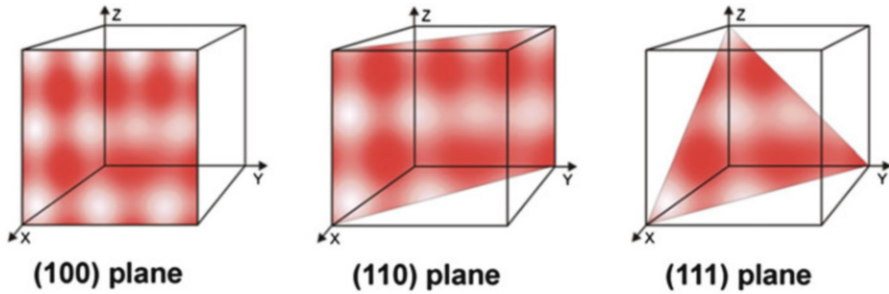
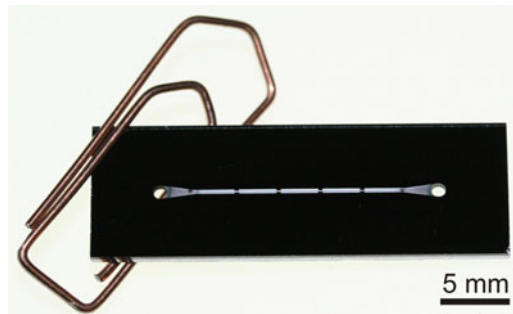


**Fig. 2.8** Position of the (100), the (110), and the (111) silicon crystal plane

**Fig. 2.9** Microfluidic system for the dispersion and emulsification of solid lipid nanoparticles made of silicon (channel bulk material) and glass (cover plate) [4]



(KOH) the etch rate of  $\{111\}$  planes is 40 times lower than that of  $\{100\}$  planes, so that the  $\{111\}$  planes can be conveniently used as etch stop. Silicon microstructures made by KOH etching therefore have always geometries dominated by  $\{111\}$  planes (see Sect. 2.6) (Fig. 2.9).

### 2.3.4 Glass

The use of glass for microsystem components, especially for microfluidic parts, implies a low coefficient of thermal expansion  $\alpha$ . Borosilicate glass with silica and boron trioxide fulfills this demand with an  $\alpha$  of around  $3 \times 10^{-6}/^{\circ}\text{C}$  at  $20^{\circ}\text{C}$  and is therefore resistant to thermal shock and less subject to thermal stress. Another outstanding advantage is that borosilicate glass can be bonded to silicon by applying a voltage of 200–1000 V (anodic bonding, see Sect. 2.8.3). As well, it can be irreversibly bonded to PDMS after oxygen plasma treatment of the PDMS and glass surfaces. Not least, borosilicate glass can be bonded to itself. To do this, the bond surfaces have to be chemically activated, aligned to each other and then exposed to mechanical load and heat. (The bonding techniques are described in detail in

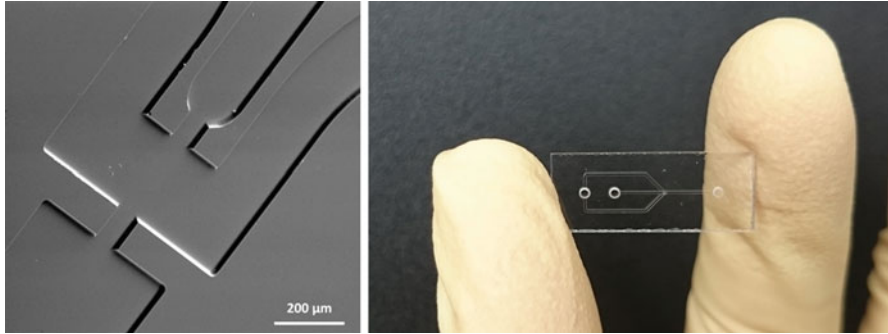


**Fig. 2.10** Microfluidic system made of glass, *left*: detail, *right*: whole system

Sect. 2.8.) Furthermore, glass can be patterned by wet chemical and dry etching techniques as well as laser ablation, so that microchannels, through-holes, cavities, etc. can be easily fabricated.

Borosilicate glass was developed by the German glassmaker Otto Schott in the late nineteenth century. In 1915 Corning Glass Works introduced Pyrex, which became a synonym for borosilicate glass in the English-speaking world [34]. In the 1990s Schott set up the first microfloat production line for the manufacture of what would soon become one of the most influential specialty glass materials. The result was a floated borosilicate glass called borofloat. Over the years borofloat has made possible a multitude of innovative products across a broad spectrum of applications in research and industry [28].

The main advantage of glass compared to other materials is its optical transparency. Moreover, it has a high Young's modulus ( $64 \text{ kN/mm}^2$  [23]), a high resistance against many acids and base and it is biocompatible and low-priced (Fig. 2.10).

Another, very interesting material for microfluidics, MEMS, and MOEMS is the photosensitive glass called Foturan manufactured by Schott AG as well. Foturan is a lithium–potassium glass dotted with small amounts of silver and cerium oxides. This material combines the unique glass properties like transparency, hardness, chemical, and thermal resistance with the opportunity to achieve very fine structures with tight tolerances and high-aspect ratio. Smallest structures of  $25 \text{ μm}$  are possible with a roughness of  $1 \text{ μm}$  [6]. The microstructures are transferred by UV light at a wavelength between 290 and 330 nm, whereby the exposed regions become crystalline. The exposure can either be done by a direct laser writing process or a mask-based exposure method. Afterwards, Foturan is etched with a 10 % solution of hydrofluoric acid at room temperature. The etching is anisotropic (see Sect. 2.6), however, the crystallized regions have an etching rate up to 20 times higher than the vitreous regions. To enlarge the aspect ratio, the etch process can be supported by ultrasound. Either structured or unstructured individual parts of Foturan may be connected without any intermediate layer by thermal diffusion bonding.

### 2.3.5 *Non-metal Thin Films*

Silicon bulk micromachining is closely linked with thin silicon oxide ( $\text{SiO}_2$ ) and silicon nitride ( $\text{Si}_3\text{N}_4$ ) layers. Thin means in the range of a few hundred nanometers. Both of them are excellent insulating materials, often used in connection with semiconductor devices like resistors, capacitors, transistors, etc. On the other hand, both materials can be used as masking layers for silicon etching. They can be patterned photolithographically and etched in buffered hydrofluoric acid solution ( $\text{SiO}_2$ ) and in phosphoric acid at  $180^\circ\text{C}$  ( $\text{Si}_3\text{N}_4$ ). The deposition of  $\text{SiO}_2$  and  $\text{Si}_3\text{N}_4$  is addressed in Sect. 2.4.1.

### 2.3.6 *Metals*

Metals are another important material group for the development of MEMS and MOEMS including microfluidic systems. Metallic conductor lines as well as masking and adhesion layers are thin-film deposited (see Sect. 2.4.2) and photolithographically patterned (gold, copper, aluminum, chrome, titanium). Thicker metallic components like electromagnetic coils (copper), magnetic field conducting structures (nickel iron), and microstamps (copper, Fig. 2.11) are usually electroplated (see Sect. 2.4.3). In microfluidic applications with high working pressures bulk stainless steel is a better choice than silicon or glass. In principle, stainless steel can be wet chemically etched, but the etch rate is rather low. However, a challenging processing method is microelectrical discharge machining ( $\mu\text{EDM}$ , see Sect. 2.9.5), which makes it possible to fabricate wear-resistant emulsifying and dispersing systems (Fig. 2.12).

**Fig. 2.11** Copper stamp for die-sinking  $\mu\text{EDM}$

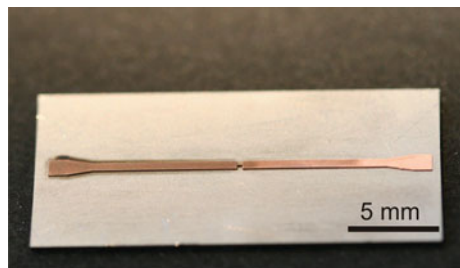
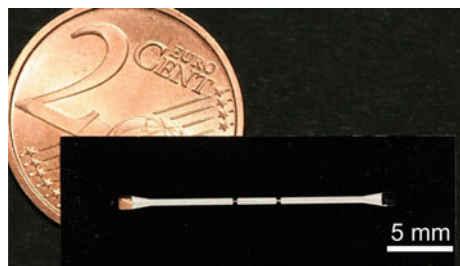


**Fig. 2.12** Microfluidic system made of stainless steel by the use of  $\mu\text{EDM}$



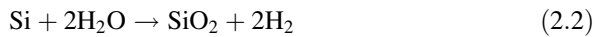
## 2.4 Deposition Techniques

### 2.4.1 Deposition Techniques for $\text{SiO}_2$ and $\text{Si}_3\text{N}_4$

Silicon oxide ( $\text{SiO}_2$ ) can be deposited with mainly two different methods, resulting in different layer properties. One method is thermal oxidation, requiring a pure silicon substrate.  $\text{SiO}_2$  growth involves the heating of the silicon wafer to temperatures between 1000 and 1250 °C and a stream of gaseous oxygen or steam. The silicon reacts with oxygen, so that the resulting  $\text{SiO}_2$  layer grows both into the substrate surface (45 %) and upwards (55 %) (Fig. 2.13). If the oxidation takes place under pure oxygen atmosphere, it is called a “dry” oxidation.



The oxidation is called “wet”, if the silicon reacts with water:

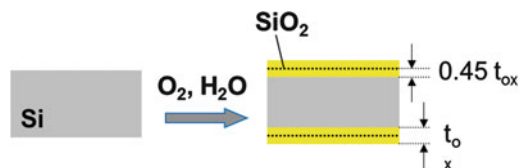


The deposition rate of the wet oxidation is higher than that of the dry one, but the quality concerning density and dielectric strength is lower. (For example, the oxide thickness of a wet process is 420 nm after 30 min at 1100 °C and 600 nm after 30 min at 1200 °C. A dry oxidation process at 1100 °C results after 30 min in a thickness of 100 nm.) At the beginning of the oxidation process, the oxide thickness is determined by the reaction rate and is linearly dependent on the oxidation time. With the passing of process time, the oxide growth is limited by the diffusion of oxygen atoms through the already existing  $\text{SiO}_2$  layer and is proportional to the square root of the oxidation time.

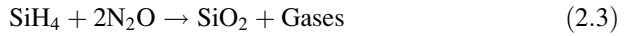
An alternative process to create thin  $\text{SiO}_2$  films but at significant lower temperatures and on nearly arbitrary substrates is the plasma-enhanced chemical vapor deposition (PE CVD). CVD processes are characterized by constituents of a vapor phase, often diluted with an inert carrier gas, reacting at a hot surface to deposit a solid film [16]. The reaction mechanism consists of several steps:

1. Gas phase reaction of reactants
2. Transport of the reaction products to the substrate surface
3. Surface reaction after adsorption of the reaction products
4. Desorption and mass transport of by-products

**Fig. 2.13** Oxide growth at thermal oxidation



Energy to drive the surface reaction can be thermal and/or be supplied by photons, electrons, or ions. In case of the PE CVD process, the plasma (an ionized gas) is the main energy provider. The process temperature can therefore be rather low. To deposit  $\text{SiO}_2$  the reactants are silane ( $\text{SiH}_4$ ) and nitrous oxide ( $\text{N}_2\text{O}$ ). The basic differences between the thermal and the plasma-enhanced oxidation are concluded in Table 2.1.



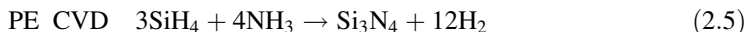
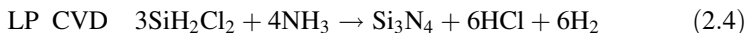
Silicon nitride  $\text{Si}_3\text{N}_4$  can be deposited by two different CVD processes: Using a low pressure and, like  $\text{SiO}_2$ , a plasma-enhanced CVD process (LP CVD and PE CVD; the main differences between them are listed in Table 2.2). The LP CVD process takes place in a vertical diffusion furnace (Fig. 2.15). The chemical reactions for both of them are as follows:

**Table 2.1** Comparison of thermal  $\text{SiO}_2$  and PE CVD  $\text{SiO}_2$

Process conditions/ layer properties	Thermal $\text{SiO}_2$	PE CVD $\text{SiO}_2$
Process temperature	800–1200 °C	<300 °C
Deposition rate	3 nm/min (dry oxidation)–20 nm/min (wet oxidation)	55 nm/min
Pressure	Atmospheric pressure	$4 \times 10^{-4}$ bar
Substrate material	Silicon	Every material withstanding the process temperature
Standard layer thickness	<1 $\mu\text{m}$	Some hundred nm
Defect density	Low	High
Dielectric strength	High	Lower
One-sided/double-sided deposition	Double-sided deposition	One-sided deposition

**Table 2.2** Comparison of LP CVD and PE CVD  $\text{Si}_3\text{N}_4$

Process conditions/ layer properties	LP CVD $\text{Si}_3\text{N}_4$	PE CVD $\text{Si}_3\text{N}_4$
Process temperature	770 °C	300 °C
Deposition rate	2 nm/min	100 nm/min
Pressure	$3.7 \times 10^{-5}$ bar	$8.7 \times 10^{-4}$ bar
Substrate material	Any material withstanding the process temperatures	Any material withstanding the process temperatures
Standard layer thickness	100 nm	300 nm
Defect density	Low	High
One-sided/double-sided deposition	Double-sided deposition	One-sided deposition



### 2.4.2 Deposition Techniques for Thin Metal Layers

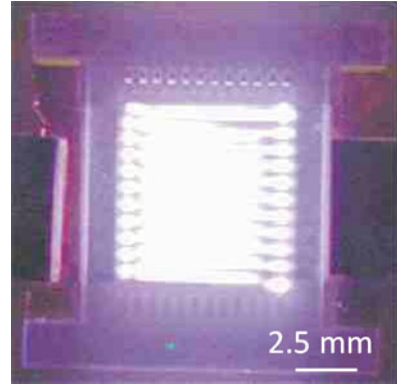
Thin metal layers are usually deposited with a physical vapor deposition (PVD) technique. The oldest PVD technique is the thermal evaporation. Evaporation is based on the boiling off or sublimating of a heated material and its subsequent condensation on a substrate. An evaporation unit consists of a vacuum chamber, an evaporation source, an aperture to control the particle stream and a substrate holder. The evaporation is a quite simple and cheap technique, but the generated thin films are inhomogeneous and the deposition rate varies considerably. Another disadvantage is that the material to be evaporated has to have a lower melting point than the crucible, limiting the range of film materials. To overcome these disadvantages, the material can alternatively be heated by electron beam or laser radiation. But these machines are more complex and therefore more expensive. Suitable metals to be evaporated are silver, aluminum, gold, chrome, nickel, titanium, and platinum. Alloys are less suitable, because their stoichiometry is difficult to control, particularly if the alloy components have different melting points and therefore different deposition rates.

Another popular PVD vacuum technique is the sputtering. The material to be deposited in the form of a target (some centimeter thick disk) is bombarded with positive argon ions. The ions are created in a plasma and accelerated to the target due to a high electric direct-current voltage (the target is on negative potential, the substrate and the vacuum chamber walls are on positive potential). The impulse of the ions is transferred to the target atoms (similar to the start of a billiard game, where a billiard ball is hit into the group of the other balls), and as a result, uncharged target atoms are released and accelerated. The direction of acceleration is more or less arbitrary, so that the atoms touch down not only on the opposite substrate but also on the walls of the recipient, where they condensate. Sputtering with alternating current voltage is usual as well, but not absolutely necessary with conducting materials like gold, copper, chrome, aluminum, tin, nickel, titanium, platinum, and even alloys. Compared with evaporation, sputtering has some obvious advantages due to a wider variety of thin film materials, a better step coverage, and a usually better adhesion to the substrate.

### 2.4.3 Deposition Techniques for Thick Metal Layers

In microfluidics, thick metal structures are not very widely used. One example is a microplasma reactor, developed and fabricated at the IMT (Fig. 2.14, [2, 29]). The reactor made of nickel can be used for the decomposition of waste gas. Another

**Fig. 2.14** Glowing microplasma reactor made at the IMT [29]



example is a copper die, which is used for die-sinking electrical discharge machining (see Sects. 2.3 and 2.9).

Microstructured thick metal layers are usually made by electroplating, that uses electric current to reduce dissolved metal cations by gaining electrons so that they generate a metal coating on an electrode (cathode). The substrate is first deposited (e.g., by sputtering) with a thin metal layer, the so-called seed layer. In a second step, an inverse mold of the metal structures is fabricated out of photoresist (SU-8 or AZ) using depth lithography (see Sect. 2.5). In the subsequent electroplating step, nickel, copper, or gold is plated upward from the seed layer into the voids left by the photoresist. Taking place in an electrolytic cell, the current density, temperature, and solution are carefully controlled to ensure proper plating. In the case of nickel deposition from  $\text{NiCl}_2$  in a  $\text{KCl}$  solution,  $\text{Ni}$  is deposited on the cathode (metalized substrate) and  $\text{Cl}_2$  evolves at the anode [12]. The resist either remains in the interstitials to isolate the metal structures from each other or it is stripped after electroplating.

## 2.5 Lithography

### 2.5.1 Photolithography

Photolithography has been employed for pattern generation in manufacturing of ICs, microchips, and MEMS devices. It is based on the exposure of light-sensitive polymers (photoresists), which are reactive to ultraviolet (UV) light with wavelengths in the range of 193–436 nm. The pattern transfer can be parallel through a mask that consists of opaque features on a transparent substrate or serially (direct writing) with a focused beam. The exposure causes the photoresist to be chemically modified, so that the exposed areas either become soluble in the subsequent developing step (positive tone photoresist) or becomes insoluble (negative tone resist) (Fig. 2.15). The patterned photoresist layer serves for example as masking



**Fig. 2.15** Difference between positive and negative tone photoresist

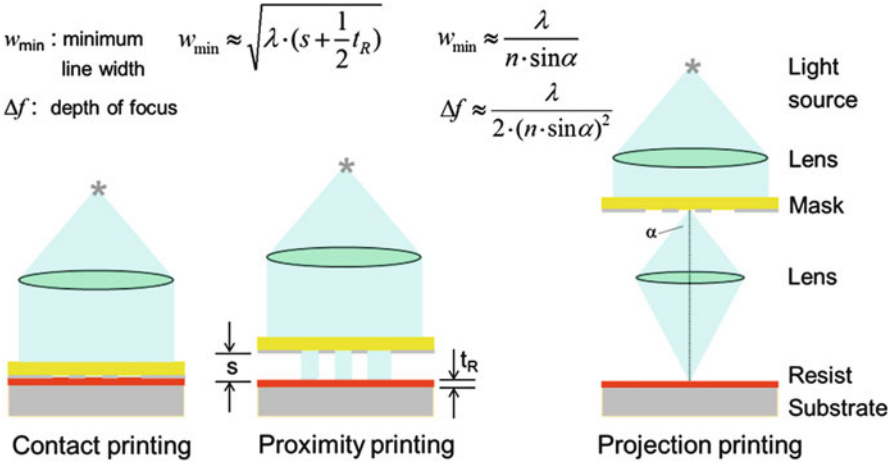
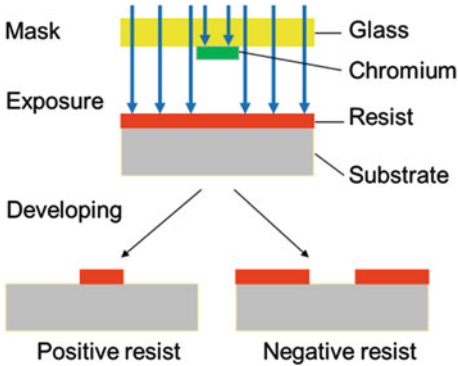


**Fig. 2.16** Three methods of photolithography printing

layer in a following etch process. The resist protects the subjacent material against the etching, so that only the unprotected areas are etched. After the etch step the resist is usually removed. Another possible use for the patterned photoresist layer is a lift-off process. A thin metal layer is therefore deposited on the exposed and developed resist. Afterwards both layers are removed together. The metal remains in the resist openings.

The mask-based pattern transfer (the printing) can be performed in three different ways (Fig. 2.16): (1) the mask is in direct contact to the resist-deposited substrate (contact printing), (2) there is a small proximity distance  $s$  between resist surface and mask (proximity printing) and (3) the mask structures are projected onto the resist through an optical system (projection printing). Table 2.3 shows the main advantages and disadvantages of the three printing methods.

**Table 2.3** Advantages and disadvantages of the three printing methods

	Contact printing	Proximity printing	Projection printing
Advantages	Very low minimum line width $w_{\min}$	Mask and resist damage and contamination is avoided	Lowest minimum line width $w_{\min}$
	No resolution reduction due to diffraction and refraction at slit		Mask and resist damage and contamination is avoided
	High throughput		High throughput
	Low cost		
Disadvantages	High risk of mask and resist damage and contamination	Larger minimum line width $w_{\min}$	Equipment much more expensive
	Defects impact	Resolution is reduced due to diffraction and refraction at slit	
Examples of use	Very small or precise structures	Sensitive or sticky resists	Enlargement or reduction of the geometry

Mask aligner can be normally used for both, the contact and the proximity printing, and are used in most microfabrication research laboratories and many low-volume production facilities. The mask aligner is an alignment and exposure tool, adjusting the mask to a substrate (wafer) with submicron precision and providing the UV light source. Usually, only the upper side of the wafer is exposed. Therefore, mask and wafer are successively loaded into the mask aligner. Both are bearing alignment marks like register crosses, which are then precisely aligned to each other by means of a top side microscope. Some mask aligners are equipped as well with a backside microscope, which allows the alignment of the loaded mask to the already exposed and developed or even patterned back side of the wafer. Another feature of the backside microscope is the alignment of transparent substrates, if they have alignment marks on their back side. After exposure, the wafer is unloaded and developed. The complete photolithography process is shown in Fig. 2.17.

### 2.5.2 Depth Lithography

Depth lithography has its origin in LIGA technology (LIGA is a German acronym for Lithography, Galvanoformung, Abformung = Lithography, Electroplating, Molding). The LIGA starts in the early 1980s with X-rays, produced by a synchrotron to create high-aspect ratio structures. The X-rays made this

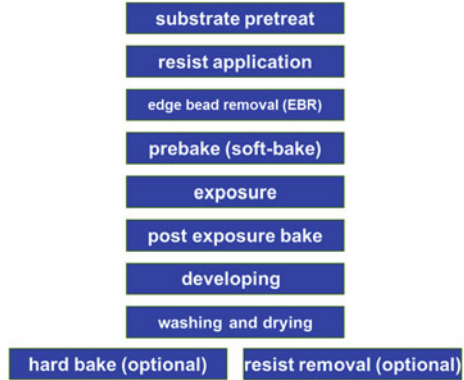
surface cleaning	Removal of particulates, organic films, adsorbed metal ions from the wafer surface
adhesion promoter application	Sometimes necessary to achieve better adhesion of the resist
resist application	Resist thickness varies with rotational speed of the spinner and viscosity of the resist
prebake (soft-bake)	70°C–90°C, necessary to drive solvents out of the resist
exposure	Contact/proximity printing, projection printing
developing	Negative tone resist: solvent; positive tone resist: alkaline developer
postbake (hard-bake)	90°C–140°C, necessary to increase both adherence and etch resistance
etching/deposition	
resist removal	Stripping solutions, plasma etching in oxygene atmosphere

Fig. 2.17 Complete photolithography process flow

technology very equipment and cost intensive. Due to the development of special UV-sensitive polymer photoresists like SU-8 (see Sect. 2.3) the depth lithography becomes highly interesting for a broader user group. After substrate pretreatment (cleaning and drying) the so-called “Poor man’s LIGA” starts with a two-step spin on process of the resist considering the recommended coating conditions [23]. The build-up of photoresist occurring at the edge of the substrate has to be removed or leveled after coating. This is done either by edge bead removal (EBR) or by leveling the wafer on a plane plate covered with a glass slid for up to half an hour. Then a pre-bake (also called soft-bake) is carried out. The next step is the exposure. The optimal exposure dose depends on the layer thickness and varies from 4 to 8 mJ/(cm<sup>2</sup> μm). The chemical transformation process of SU-8 to become insoluble is described in Sect. 2.3. To enhance the cross-linking process, a second thermal treatment, the PEB, has to take place directly after exposure. The PEB is followed by the developing under strong agitation. The last steps of photolithography are washing and drying. For washing fresh developer, 2-propanol is used. By contact with 2-propanol, undeveloped SU-8 will form a white haze. In this case, the development was not finished and needs to be continued. Afterwards the wafer is rinsed with DI-water and dried in a spin drier or by nitrogen stream.

If the developed resist is to be left as part of the final device and if this device is to be subjected to thermal load, a hard bake has to be incorporated into the process. It is recommended to use a final bake temperature 10 °C higher than the maximum expected device-operating temperature. However, the removal of fully cross-linked resist is extremely difficult. Recommended removal methods are plasma stripping, etching with piranha etch, laser ablation, and pyrolysis (Fig. 2.18).

**Fig. 2.18** Complete depth lithography process flow



## 2.6 Etching Techniques

### 2.6.1 Characteristics of Etching Processes

There are two main parameters to characterize etching processes: The selectivity  $S$  and the anisotropy  $A$ . The selectivity is the etch rate relation of different materials. A typical example of a treble etch system, shown in Fig. 2.23, is: (1) substrate, (2) layer to be etched, and (3) masking layer. The layer to be etched should have a high etch rate, whereas both the substrate and the mask layer should have a much lower etch rate. In other words, the selectivity should be as high as possible. Table 2.4 shows some exemplary double etch systems, common etch solutions, etch rates of both materials, and the resulting selectivity  $S$  [3].

The anisotropy  $A$  is the relation between the lateral and the vertical etch rate.

$$A = 1 - \frac{v_l}{v_v} \quad (2.6)$$

$v_l$ : lateral etch rate

$v_v$ : vertical etch rate

If  $A = 0$  the etch process is fully isotropic (etch rates are equal in all directions). If  $A = 1$  it is anisotropic (etch rate direction dependent) (Fig. 2.19).

### 2.6.2 Wet Chemical Etching of Thin Films

Most of the common thin film materials ( $\text{SiO}_2$ ,  $\text{Si}_3\text{N}_4$ , and metals) can be etched by chemical solutions. Normally, the wet etching processes are isotropic. In case of thin films ( $<1 \mu\text{m}$ ) the resulting undercutting of the mask layer reduces the

**Table 2.4** Selectivity of some exemplary etch systems

Etch system	Etch solution	Average etch rate relation [nm/min]	Selectivity, <i>S</i>
SiO <sub>2</sub> :Si	Buffered hydrofluoric acid NH <sub>4</sub> F + HF + H <sub>2</sub> O	200:2	ca. 100
Si <sub>3</sub> N <sub>4</sub> :SiO <sub>2</sub>	Hot phosphoric acid H <sub>3</sub> PO <sub>4</sub>	10:1	ca. 10
Poly-Si:SiO <sub>2</sub>	Nitric acid HNO <sub>3</sub> + hydrofluoric acid HF + acetic acid CH <sub>3</sub> COOH	150:10	ca. 15
Al:SiO <sub>2</sub>	Phosphoric acid H <sub>3</sub> PO <sub>4</sub> + acetic acid CH <sub>3</sub> COOH + nitric acid HNO <sub>3</sub> + H <sub>2</sub> O	35:0.7	ca. 50

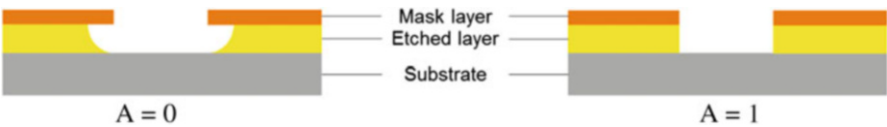


**Fig. 2.19** Isotropic etching (*left*) and anisotropic etching (*right*)

resolution, but can be generally neglected (Fig. 2.19, left). To be wet chemically etched, the wafer is either dipped into an etch bath or sprayed with the etch solution.

2.6.3 Isotropic Wet Chemical Etching of Glass and Silicon

Solutions for isotropic wet etching of glass and silicon are usually hydrofluoric acid (HF) based. The glass etching solution contains varying hydrofluoric acid concentrations or solutions combining HF with other strong acids like HCL, HNO<sub>3</sub>, H<sub>2</sub>SO<sub>4</sub>, or H<sub>3</sub>PO<sub>4</sub> to enhance the etch rate [12]. The mask layer is usually a combination of chromium (to enhance the adhesion) and gold or alternatively photoresist, which saves some process steps but bears the risk of less reliable adhesion. For isotropic etching of silicon a solution consisting of HF, HNO<sub>3</sub>, and NH<sub>3</sub>COOH, called HNA (hydrofluoric, nitric, acetic) solution, in combination with a mask layer made of SiO<sub>2</sub> is used.

Both, the isotropic wet etching of silicon and glass are generally used to achieve large etching depths, so that the isotropic etch behavior has to be considered in determining the mask design.

2.6.4 Anisotropic Wet Chemical Etching of Silicon

As already mentioned in Sect. 2.3 single-crystalline silicon is characterized by its anisotropic (crystal plane dependent) behavior, also relating to the etch rates in specific etch solutions. The different etch rates of the crystal planes can be

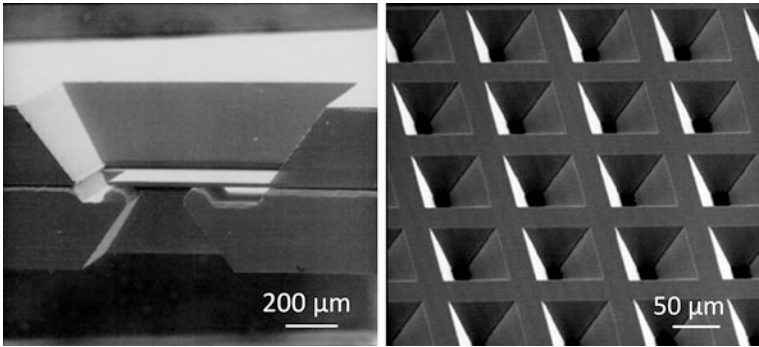


**Fig. 2.20** Silicon bulk microfluidic devices: passive valve (*left*) and silicon grid (*right*)

**Table 2.5** Etch rates of the {100}, {110}, and {111} planes of single crystal silicon in 40 % KOH solution at 80 °C

Crystallographic plane	Etch rate
{100}	1 μm/min
{110}	2 μm/min
{111}	0.03 μm/min

excellently used for building three-dimensional mechanical and fluidic microdevices (wet bulk micromachining). In Fig. 2.20, the left scanning electron microscope SEM picture shows a passive microvalve consisting of an upper and a lower part bonded together. The valve is normally closed. It opens, when the fluid pressure causes the beam to bend up and closes again, when the fluid pressure falls below a defined limit. The second exemplary silicon bulk device is a grid, which can be used as reactor unit (Fig. 2.21, right).

A well-known etch solution for anisotropic wet chemical etching of silicon is potassium hydroxide solution ( $\text{KOH} + \text{H}_2\text{O}$ ) at a temperature of about 80 °C. In this case, anisotropy refers to the etch rate relation of different crystal planes, concretely those of the {100}, {110}, and {111} planes (Table 2.5).  $\text{SiO}_2$  or  $\text{Si}_3\text{N}_4$  are used as mask layers.

Thus, the anisotropy of {100}:{110}:{111} is about 40:80:1. In practice, the {111} planes are used as etch stop layers. Because of the angles between the (100) plane and the (110) respectively the (111) plane characteristic geometric structures are formed, as can be seen in Fig. 2.21a and b.

(100) wafers are used to etch indentations, cavities, and holes and to fabricate thin membranes. The sidewalls are always pyramid-shaped, the bases rectangular or square. With (110) wafers long, narrow channels with vertical sidewalls are fabricable. To conclude, the anisotropic wet chemical etching of silicon with, for example, KOH solution is very simple and cost saving concerning the process guiding and the equipment. But there are massive restrictions in terms of geometric forms impeding the design of microsystems.

Further solutions for anisotropic etching of silicon are tetramethylammoniumhydroxide (TMAH  $\text{C}_4\text{H}_{13}\text{NO}$ ) and ethylenediaminpyrocatechol (EDP,  $\text{C}_2\text{H}_8\text{N}_2 + \text{C}_6\text{H}_6\text{O}_2 + \text{H}_2\text{O}$ ). The anisotropy of both of them is lower than of KOH.

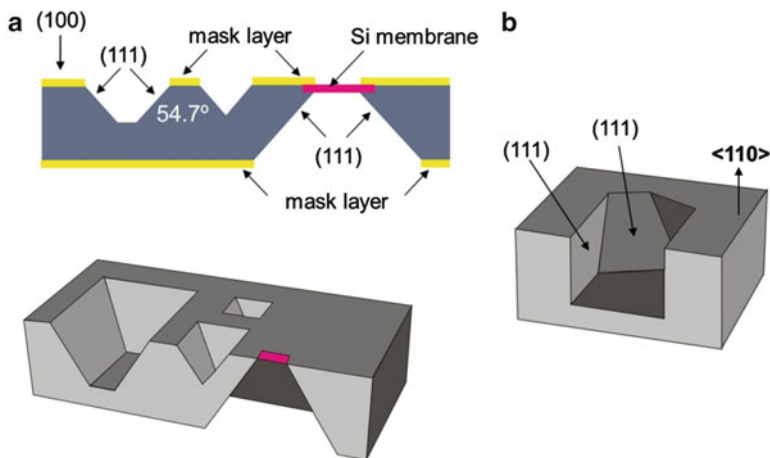


**Fig. 2.21** (a) Silicon wafer with a (100) plane as surface etched in KOH solution. The (111) etch stop plane and the (100) plane stand at an angle of  $54.7^\circ$  to each other, resulting in pyramid-shaped holes (*above*: sectional view, *below*: 3D sketch). (b) Schematic 3D view of a (110) wafer etched in KOH solution. The angle between the (110) and the (111) plane is  $90^\circ$ , resulting in vertical side walls, and  $35.26^\circ$  as well

### 2.6.5 Dry Etching Techniques

If the etch process takes place in gaseous atmosphere, it is called “dry”. There are pure chemical and pure physical mechanisms as well as combinations of both with different stakes (Table 2.6).

An alternative to KOH etching of silicon is the deep silicon reactive ion etching (Deep RIE or DRIE). It is based on an advanced silicon etching process, which has been originally developed and patented by the Robert Bosch GmbH in Stuttgart, Germany. This process alternates repeatedly between a nearly isotropic plasma etch step and the deposition of a chemically inert passivation layer. This etch technique provides nearly  $90^\circ$  sidewall profiles with any basic form. The etch rate is roughly the same as with KOH, and, as an advantage, photoresist is suitable as mask layer. If the energy to generate reactive ions is coupled inductively, it is also called ICP etch process.

The DRIE process can also be used for deep etching of glass. Fluidic channels and vias with high-aspect ratios as they are not practical in the more popular wet chemical etching process (Sect. 2.6.3) can be fabricated in the same devices like silicon dry etching. Here, gases like  $\text{SF}_6$ ,  $\text{C}_4\text{F}_8$ , and  $\text{CHF}_3$  are used for chemical etching. In the plasma the gas is ionized into fluorine and carbon radicals, which are accelerated towards the glass substrate. There fluorine radicals react with Si-atoms of the glass and carbon ions with the  $\text{O}_2$  respectively to volatile compounds to be pumped out of the chamber. Additional gases like  $\text{O}_2$ ,  $\text{H}_2$ , Ar, or He improve the stability and selectivity of the process, too [15]. Never the less, the selectivity is one

**Table 2.6** Dry etching technologies

Techniques	Materials to be etched	Mechanism	Etch species	Etch profile	Selectivity
Barrel etching	Silicon, silicon nitride $\text{Si}_3\text{N}_4$	Chemical reaction	Reactive radicals diffuse to the substrate surface	Isotropic ( $A = 0$ )	High
Plasma etching (PE)	Semiconductor materials, metals, dielectrics, polymers	Combination of physical and chemical mechanisms; the physical stake increases top down	Reactive radicals with less ion bombardment	Rather isotropic	Lower
Reactive ion etching (RIE)	Silicon, glass, any organic matter		Reactive radicals and reactive ions	Rather anisotropic	Less
Reactive ion beam etching (RIBE)	Gallium arsenide, indium phosphide, cadmium mercury telluride		Reactive ions		
Ion beam etching (IBE), focused ion beam etching (FIB)	In general no restrictions (all metals, all semiconductor materials)	Physical bombardment	Non-reactive ions	Anisotropic ( $A = 1$ )	Low
Sputter etching	No restrictions; mainly used to clean the substrate surface before sputtering				

of the main issues and therefore a proper masking layer is important. Electroplated nickel, chrome, silicon, SU-8, and resist have been used as masking material [14].

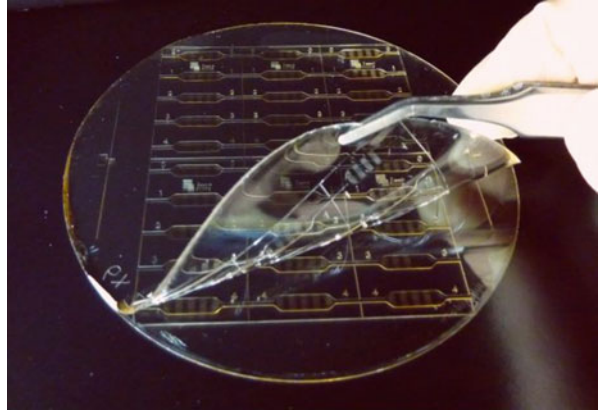
## 2.7 Second Cast Techniques

### 2.7.1 Soft Lithography

To call this technique “soft lithography” is, however, misleading; it is in fact a non-photolithographic method for replicating a pattern. The result is a device made of PDMS (see Sect. 2.3) or other elastomeric (soft) materials. Rigid masters serve as pattern transfer agents. These masters can be made of a variety of materials. One of the most popular master materials is SU-8 (Sect. 2.3), which is photolithographically structured. To fabricate the PDMS replica, the siloxane oligomer and the



**Fig. 2.22** Peeling off a PDMS layer. The master structure is made of SU-8 [5]



curing agent are mixed (usually in a ratio of 10:1) and afterwards degassed in a vacuum chamber. Then, the PDMS pre-polymer is poured over the master structure. The PDMS conforms to the shape of the master and replicates its features with high resolution. As already mentioned in Sect. 2.3 the cross-linking of PDMS can take place at room temperature, but is accelerated by enhancing the temperature (e.g., 70 °C for 60 min). The PDMS can then be peeled off the master structure (Fig. 2.22).

Soft lithography is a low-cost and effective method to fabricate PDMS micro- and nanostructures for microfluidic purposes.

### 2.7.2 Injection Molding

Macroscopic injection molding is a well-known technology, which enables a low-cost mass production of thermoplastic polymer devices. To fabricate micro-scale devices, a variotherm process has to be applied. Therefore, the two-part mold cavity with the micromold insert is closed, evacuated, and heated above the glass transition temperature of the polymer [13]. The polymer is heated as well to become viscous and is pressed into the mold. Both, the mold tool and the polymer are then cooled down below its glass transition temperature. Finally, the polymer workpiece is demolded and reworked if necessary. In general, cycle times are shortest when producing micro parts from polymers by injection molding. A disadvantage is the complex micromold insert, which can be fabricated for example by microelectrical discharge machining  $\mu$ EDM (see Sect. 2.9). A selection of thermoplastic polymers for injection molding is listed in Table 2.7.

Recent research activities include the development and design of micromold inserts, the fabrication, and processing of unfilled and magnetically soft ultrahigh-filled polymers, the characterization of the polymer's flow behavior, the investigation of weld lines, and the simulation of the melt distribution [36].

**Table 2.7** Thermoplastic polymers for injection molding

Acronym	Full name
PMMA	Polymethylmethacrylate
PC	Polycarbonate
PS	Polystyrene
POM	Polyoxymethylene
PVC	Polyvinylchloride
PP	Polypropylene
PEEK	Polyetheretherketone
PA	Polyamide
PVDF	Polyvinylidene fluoride

## 2.8 Bonding Techniques

### 2.8.1 In General

Bonding of two or more microstructured components aims to create closed fluid channels, sealed cavities, and complex 3D structures. Furthermore, it can be used to strengthen the mechanical stability and to generate a thermal coupling or decoupling, an electrical contact, a galvanic separation, and the interface to the surrounding periphery.

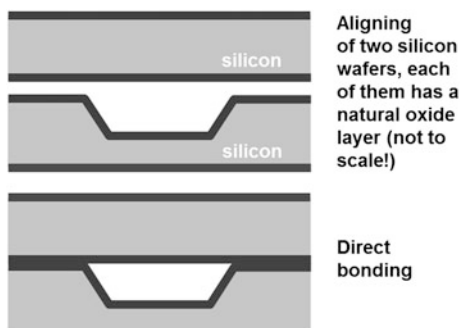
Mainly, bonding takes place on wafer-level. Depending on the materials of the bond partner, commonly used techniques are the silicon direct bonding, the anodic bonding, the thermal bonding, the plasma-activated bonding, and the bonding with intermediate layers (solid–liquid interdiffusion bonding, adhesive bonding, glass frit bonding).

### 2.8.2 Silicon Direct Bonding

Two silicon wafers can be bonded by thermal treatment without any additional intermediate layers (Fig. 2.23). The so-called silicon direct bonding SDB is based on intermolecular interactions. Because of the necessary particle freedom of the bond surfaces, at first both wafers have to be cleaned very carefully. The RCA clean, which has been developed by Werner Kern at RCA laboratories, also creates hydrophilic surfaces with hydroxyl ( $\text{OH}^-$ ) groups. After being cleaned, the silicon wafers are aligned and prebonded. The prebond, which is already quite stable but reversible, is induced by the bonding of the OH-groups and by Van der Waals forces. The wafers are then annealed in  $\text{N}_2$  or  $\text{O}_2$  atmosphere at a temperature above  $800^\circ\text{C}$ . Thereby hydrogen  $\text{H}_2$  is freed from the OH-groups and diffuses out leaving silicon–silicon and silicon–oxygen bonds.

Because of the compatibility of silicon to medical and chemical application areas, silicon direct bonding is mainly advantageous due to the absence of other materials. But the requirements concerning flatness and cleanliness of the bond surfaces in combination with high process temperatures make this bonding technique very demanding.

**Fig. 2.23** Silicon direct bonding (sectional view of the two wafers)



### 2.8.3 Anodic Bonding

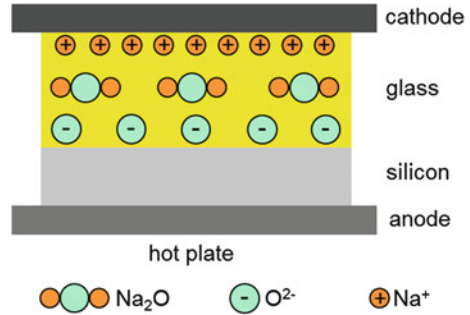
With the objective to provide a bond technique without any additional bond material but at considerably lower process temperatures the anodic bonding has been introduced. This technique is a type of field assisted or electrostatic bonding and demands borosilicate glass (pyrex or borofloat, see Sect. 2.3) and either silicon or metal as bond partners. Anodic bonding of two silicon wafers is only feasible if a glass layer is deposited on one of them. For medical or biological applications glass is suitable as well, so that the combination of glass and silicon is no general disadvantage; quite the contrary, glass is due to its transparency in many cases even more suitable. Furthermore, the above-mentioned glass types have a thermal expansion coefficient  $\alpha$  quite similar to silicon, so that mechanical stress is avoided as far as possible.

For anodic bonding a process unit generating an electric field is necessary. Again, the silicon and the glass wafers are carefully cleaned and prebonded at first. Then they are placed on a heated bond chuck (350–450 °C) and a high negative voltage of 200–1000 V is applied to the glass side. Due to the heating, the positive sodium ions  $\text{Na}^+$  (borosilicate glass contains app. 4 % by weight  $\text{NaO}_2$ ) become mobile and drift towards the cathode. Therefore, a depletion region is formed at the Si/glass interface, resulting in a high electric field force generating stable intimate contact (Fig. 2.24). The oxygen ions  $\text{O}^{2-}$  bond to the silicon forming a hermetic seal.

### 2.8.4 Glass Bonding

Microfluidic channels fabricated from glass provide a transparent, chemical and temperature-stable system. Hence, the bonding has to keep these properties in the final fluidic chip. By thermal bonding of two glass wafers no additional material

**Fig. 2.24** Schematic of anodic bonding



like polymers, which are often opaque and not that chemical stable-like glass, is needed. Essential for a successful bond between two glass wafers is that both have the same thermal expansion coefficient and similar glass transition temperature [10]. Therefore bonding of identical glass type is preferred. Before bringing the surfaces in contact, each wafer has to be cleaned properly and activated by O<sub>2</sub>-plasma or piranha treatment (peroxymonosulfuric acid H<sub>2</sub>SO<sub>5</sub>). This ensures the presence of sufficient OH-groups at the surface. Presence of Newton's rings after the prebond is an indicator for insufficient cleaning. In this case, the wafers have to be separated again and cleaning has to be repeated. The bonding itself takes place in a (vacuum) furnace at 500–650 °C for several hours. The result is a chemical and temperature stable bonding, which can withstand even high pressures [25, 32].

### 2.8.5 Plasma-Activated Bonding

Plasma activation of bond surfaces enables the direct bonding to be operated at lower temperatures. The plasma causes the removal of contaminants, the generation of Si–OH groups, and hence the hydrophilization of the surface, the enhancement of viscous flow of the surface layer, and the enhanced diffusivity of water at the interface. For microfluidic systems, the bonding of PDMS to itself or to other materials like glass, silicon, silicon oxide, silicon nitride, and SU-8 is a common task. The plasma treatment of the PDMS surface, which can for example take place in a barrel etcher, converts the methyl (–OSi(CH<sub>3</sub>)<sub>2</sub>O–) groups to silanol (–O<sub>n</sub>(Si(OH)<sub>4–n</sub>) groups, resulting in a hydrophilic surface with polar characteristics [8]. The hydrophilization of glass is equivalent. A condensation reaction, leading to the formation of covalent siloxane (Si–O–Si) bonds, leads to the irreversible bonding of two plasma-activated surfaces. In case of other bond partners the contamination removal (inorganic materials), and the introduction of polar functional groups (organic polymers) are the leading effects.

## **2.8.6 Bonding with Intermediate Layers**

### **2.8.6.1 Solid–liquid Interdiffusion Bonding**

The solid–liquid interdiffusion bonding (SLID) is based on rapid formation of intermetallic compounds (IMC) between two metal components: one low-temperature melting component (e.g., Sn) and one high-temperature melting component (e.g., Cu or Au). The bonding is typically carried out at moderate temperatures between 250 and 300 °C, which is above the melting point of Sn. When the Sn melts, the IMCs solidify isothermally. For correctly designed layer thicknesses, the resulting bond-line will only consist of Cu and the intermetallic phases ( $\text{Cu}_6\text{Sn}_5$  and  $\text{Cu}_3\text{Sn}$ ), with melting temperatures of 415 °C and 676 °C, respectively. The overall goal of the wafer-level bonding process is to achieve a Cu/ $\text{Cu}_3\text{Sn}$ /Cu final bond-line, which is thermodynamically stable [21]. The advantages of SLID bonding are high temperature stability, oxidation resistance, relatively low-processing temperatures, and high mechanical robustness. Disadvantageous is that the technology is still relatively unexplored and in case of using gold quite expensive.

### **2.8.6.2 Adhesive Bonding**

An appropriate method to bond devices of different materials, particularly new materials and new material combinations, is the adhesive bonding. This bonding technique involves glues, epoxies, or various plastic agents that bond by evaporation of a solvent or by curing a bonding agent with heat, pressure, or time [1]. The challenges of adhesive bonding are the necessary extensive knowledge of chemistry, physics, and engineering on the one hand, and the requirements to the application techniques on the other hand. The latter includes dosing and mixing techniques, the application methods themselves, and the determination of rheological properties. The main adhesives used for microsystems are epoxy resins (e.g., SU-8) and polymers (e.g., Benzocyclobutene BCB). Adverse properties of adhesive bonding are the low temperature and chemical stability as well as the medical and biological incompatibility. If the bond should be conductive, metal (nano) particles can be added to the adhesive, but the conductivity cannot be as high as in metallic connections.

### **2.8.6.3 Glass Frit Bonding**

Low melting glass is deposited onto at least one of the bond surfaces by means of screen printing. Afterwards, the glass frit is heated to an intermediate temperature, where the glass does not yet fully melt, in order to degas the organic additives. Both wafers are then aligned and charged with heat and pressure, so that the glass frit

melts completely, wetting the surface of the second wafer and creating the bond interface. Finally, the stack is cooled down under pressure. Glass frit bonding has excellent sealing performances and a high bonding strength and does not need any voltage during bonding process. Disadvantages may be the relatively large final thickness of the glass frit (10  $\mu\text{m}$ ) and the large minimum line width of about 150  $\mu\text{m}$ .

## **2.9 Maskless Patterning Techniques**

### **2.9.1 In General**

The photolithography technique as described in Sect. 2.5.1, which is highly developed and used in many areas, leaves the shortening of fabrication time to be desired. Maskless (=“digital”) techniques promise high-speed micromachining of different materials with micron resolution and are currently intensively advanced and optimized. The digital patterning techniques include laser micromachining, inkjet printing, 3D printing, microelectrical discharge machining, and machining techniques.

### **2.9.2 Laser Micromachining**

Laser radiation has some outstanding properties for micromachining: Spatial coherence, which enables maximum focusing and the generation of very high energy densities, monochromaticity, and the creation of very short, exact laser pulses. The material is removed by laser ablation, which is usually based on the absorption of laser photons. The absorption again demands a material-specific wavelength. The absorbed energy causes the material to heat up and hence to melt, evaporate, or sublime. In contrast, ultrafast lasers cause ablation as a result of multiphoton absorption at high peak intensities, so that even materials transparent to the laser wavelength can be machined.

Many types of lasers are supposed to be used for micromachining materials. These include microsecond carbon dioxide ( $\text{CO}_2$ ) lasers at wavelengths between 9.3 and 11  $\mu\text{m}$ , nanosecond and femtosecond solid-state lasers at wavelengths between 1030 and 1064 nm (e.g., Nd:YAG and Ti:Sapphire) with the possibility of higher harmonic generation in visible (515–535 nm) and ultraviolet (UV) spectrum (342–355 nm and 257–266 nm), then copper vapor lasers, diode lasers, and excimer lasers emitting at UV region (157–353 nm) [27].

Pulse duration, pulse energy, translation speed, and repetition rate are important process parameters. They influence the material removal rate and the size of the heat-affected zone and thus the quality of the microstructure. Ultra short pulse laser radiation (pulse duration in the range of pico- and femtoseconds) allows even

highly temperature-sensitive materials to be machined, because the heat input is almost nonexistent.

Moreover, glass can be patterned with high-intensity femtosecond laser pulses, which allows direct ablation of the material. Furthermore, fs-lasers can be used to modify the interior of glass in a selective manner. This is done by multiphoton absorption at the focal point of the laser beam. The chemical properties of the substrate get altered and allow selective etching in hydrofluoric acid (HF), as the etch rate of the laser-irradiated regions is several times higher than this of normal glass [31].

### ***2.9.3 Inkjet Printing***

Inkjet printing, a purely additive process, is commonly used to reproduce digital images in the form of depositing specially formulated ink onto paper or other substrates. More recently, researchers around the world are discovering innovative functional applications for inkjet printing in fields such as printed electronics, microfluidics, microoptics, life sciences, medicine, and security printing. Mainly, it has the potential to be a facile and rapid method to pattern conductive paths on rigid as well as flexible substrates or over prefabricated microstructures.

The majority of commercial inkjet printers have a piezoelectric printhead that jets an ink drop out of a nozzle, which has a diameter typically less than 40  $\mu\text{m}$ . Printable materials are

- Conductive materials (nanoparticle/precursor inks)
- Polymers
- Dielectric powders
- Dopant
- Resists
- Silicon nanoparticles
- Enzymes
- Isolating materials

However, there is still a strong need for optimizing the printheads for particle-loaded inks with the goal to avoid irreversible blockages.

### ***2.9.4 3D Printing***

3D printing has started in the twenty-first century and is an additive process of fabricating three-dimensional solid objects from a digital file. Since then there has been an enormous development of printers, filament materials, and design software, and the complexity and resolution of printed devices have been already greatly increased. In parallel the price of 3D printers has dropped substantially.

The creation of a 3D printed object is achieved by laying down successive layers of material until the entire object is created. Each of these layers can be seen as a thinly sliced horizontal cross-section of the eventual object.

The technology currently receives a lot of attention both from industry and from private persons and the areas of use seem to be nearly unlimited: industrial design, architecture, engineering, and construction (AEC), automotive, aerospace, dental and medical industries, education, toy industry, geographic information systems, civil engineering, jewelry, footwear, and many others. Microfluidic systems benefit from the low cost and time-saving possibility of printing mainly housings with integrated fluidic interfaces. Nowadays, microsystems themselves are not fabricable, because the accuracy of 3D printed devices is still too low.

### ***2.9.5 Microelectrical Discharge Machining***

Microelectrical discharge machining ( $\mu$ EDM) is a promising method for the fabrication of 3D microdevices of unconventional and wear-resistant materials. It is a non-contact material removal without process forces, and a heat affected zone is not being expected. The EDM process is based on the thermoelectric energy generated between a workpiece and a tool electrode submerged in a dielectric fluid. Both are separated only by a small gap. An electric discharge (spark-over) causes material removal by melting and evaporation. The material removal always takes place on both sides: the workpiece and the tool electrode. According to the choice of adequate process parameters it is possible to minimize the tool wear and to maximize the material removal at the workpiece. Additionally the chosen process parameters determine the achievable removal rate, process time, and surface quality. The erosion parameters depend on the material combination of workpiece and tool electrode. They have to be proved and customized for every specific application. In general, four groups of  $\mu$ EDM types can be distinguished. In microwire electrical discharge machining ( $\mu$ WEDM), a wire with a diameter of about 200  $\mu$ m is used to cut through a workpiece. The die-sinking EDM utilizes a die, which represents the negative geometry, to emboss the positive one into the workpiece. Both,  $\mu$ EDM-milling and  $\mu$ EDM-drilling use a rod electrode as tool [26].

### ***2.9.6 Micromachining Techniques***

There exists a wide variety of important applications for microsystems as well as for microfluidic devices (e.g., asymmetric high precision molds), which require high-strength materials and complex geometries that cannot be produced using current MEMS fabrication technologies. Micromachining has the potential to fill this void in MEMS technology by adding the capability of free form machining of



complex 3D shapes from a wide variety and combination of traditional and well-understood engineering materials (alloys, composites, polymers, glasses, and ceramics).

Micromachining techniques like microgrinding, microdrilling, and micromilling are downscaled from macroprocesses. Kinematically similar to conventional macromachining, micromachining is a mechanical material removal process using geometrically defined cutter edges. The size and geometry of microcutting tools determine the limit of the size and accuracy of micro devices.

Microgrinding is used to achieve high surface quality and shape accuracy of a workpiece. As an example, the usage of fine-grained diamond grinding wheels and adjusted process parameters enable to produce a surface roughness of about  $R_a = 5$  nm. The grinding process can be assisted by ultrasound, reducing the process forces [9].

The manufacturing of bores is a challenging aspect within the production chain of micro devices. When scaling down twist drills, the ratio between core size and tool diameter increases to ensure a sufficient stability. This causes a more or less unsuitable drilling process, so that the parameters usually have to be determined only by experiments. Furthermore, the chip transportation from the bottom of the bore is more complicated [9].

Micromilling is much more flexible for machining three-dimensional microgeometries. Two-edged end mills are for example made of fine grain tungsten carbide, single-edged mills consist of monocrystalline diamond. With the tungsten carbide mill microstructures with an aspect ratio of 1:24 could be realized. With monocrystalline diamond, an aspect ratio of 1:13 could be achieved anyway [8].

## References

1. Adhesives.org (2015) <http://www.adhesives.org>. Accessed 3 Aug 2015
2. Baars-Hibbe L, Sichler P, Schrader C, Geßner C, Gericke KH, Büttgenbach S (2003) Microstructured electrode arrays: atmospheric plasma process and applications. *Surf Coat Technol* 174–175:519–523
3. Büttgenbach S (1994) *Mikromechanik*. Teubner Verlag, Stuttgart. ISBN 3-519-13071-8
4. Büttgenbach S, Balck A, Demming S, Lesche C, Michalzik M, Al-Halhouli AT (2009) Development of on chip devices for life science applications. *Int J Eng* 3(2):148–158
5. Büttgenbach S, Balck A, Demming S, Lucas N, Michalzik M (2009) *Softlithografie—der schnelle Weg zum Lab on Chip*. Mikroproduktion vol 05/09, special Mikrostrukturtechnik, Carl Hanser Verlag, München
6. Caltech Engineering Design Research Laboratory (2015) Foturan<sup>®</sup> processing and properties. [www.design.caltech.edu/micro-propulsion/Foturane.html](http://www.design.caltech.edu/micro-propulsion/Foturane.html). Accessed 3 Aug 2015
7. Clarson SJ, Semlyen JA (eds) (1993) *Siloxane polymers*. Prentice Hall, Englewood Cliffs
8. Demming S (2011) *Disposable Lab-on-Chip systems for biotechnological screening*. PhD Thesis, Berichte aus der Mikro- und Feinwerktechnik, vol 30, Shaker Verlag, Aachen
9. Denkena B, Hoffmeister HW, Reichstein M, Illenseer S, Hlavac M (2006) Micro-machining processes for microsystem technology. *Microsyst Technol* 12:659–664

10. Ehrfeld W, Bähr J (2002) Handbuch Mikrotechnik: 47 Tabellen. Hanser Verlag, München Wien. ISBN 3446215069, 9783446215061
11. European Commission (2015) Eudra book V1, compendium of EU pharmaceutical law, Annex 1. ISBN 978-92-79-44435-7. doi:[10.2772/288501](https://doi.org/10.2772/288501)
12. Ferret (2015) ISO 21501: particle counters from Kenelec Scientific. <https://www.ferret.com.au>. Accessed 17 Aug 2015
13. Heckele M, Schomburg WK (2004) Review on micro molding of thermoplastic polymers. *J Micromech Microeng* 14:R1–R14. doi:[10.1088/0960-1317/14/3/R01](https://doi.org/10.1088/0960-1317/14/3/R01)
14. Henry MD (2010) ICP etching of silicon for micro and nanoscale devices. PhD Thesis, California Institute of Technology
15. Kalangutkar PK (2015) Advances in biomedical field using NEMS a fusion between MEMS and nanotechnology. *Int J Adv Res Comput Sci Softw Eng* 5(11):132–136. ISSN 2277 128X
16. Kolari K, Saarela V, Franssila S (2008) Deep plasma etching of glass for fluidic devices with different mask materials. *J Micromech Microeng* 18:064010. doi:[10.1088/0960-1317/18/6/064010](https://doi.org/10.1088/0960-1317/18/6/064010) (6pp)
17. Linear polydimethylsiloxanes. Joint Assessment of Commodity Chemicals (1994) Report no. 26. ISSN 0773-6339-26
18. Lorenz H et al (1998) Mechanical characterization of a new high-aspect-ratio near UV-photoresist. *Microelectron Eng* 41(42):371–374
19. Lucas N (2009) Microplasma stamps—an atmospheric-pressure plasma source for the area-selective modification of surfaces. PhD Thesis, Be-richte aus der Mikro- und Feinwerktechnik, vol 23, Shaker Verlag, Aachen
20. Lucas N, Demming S, Jordan A, Sichler P, Büttgenbach S (2008) An improved method for double-sided moulding of PDMS. *J Micromech Microeng* 18:075037 (5pp)
21. Luu TT, Duan A, Aasmundtveit KE, Hoivik N (2013) Optimized Cu-Sn Wafer-level bonding using intermetallic phase characterization. *J Electron Mater* 42(12):3582–3592
22. Madou MJ (2002) Fundamentals of microfabrication, 2nd edn. CRC Press, Boca Raton. ISBN 0-8493-0826-7
23. MicroChem (2015) SU-8 2000 features. Datasheet. [http://www.microchem.com/pdf/SU-82000DataSheet2000\\_5thru2015Ver4.pdf](http://www.microchem.com/pdf/SU-82000DataSheet2000_5thru2015Ver4.pdf). Accessed 3 Aug 2015
24. MicroChem Corporation (2015) NANO SU-8 negative tone photoresist formulations 2-25. <http://www.microchem.com>. Accessed 3 Aug 2015
25. Oosterbroek RE, Hermes DC, Kakuta M, Benito-López F, Gardeniers HJGE, Verboom W, Reinhoudt DN, van den Berg A (2006) Fabrication and mechanical testing of glass chips for high-pressure synthetic or analytical chemistry. *Microsyst Technol* 12:450–454. doi:[10.1007/s00542-005-0043-5](https://doi.org/10.1007/s00542-005-0043-5)
26. Richter C, Krah T, Büttgenbach S (2012) Novel 3D manufacturing method combining microelectrical discharge machining and electrochemical polishing. *Microsyst Technol* 18:1109–1118
27. Rihakova L, Chmelickova H (2015) Laser micromachining of glass, silicon and ceramics. *Adv Mater Sci Eng* 2015, Article ID 584952, 6 pages
28. Schott (2015) Borofloat. Inspiration through quality. [www.schott.com/borofloat](http://www.schott.com/borofloat). Accessed 3 Aug 2015
29. Sichler P (2006) Mikrostrukturierte Fingerelektroden als Plasmaquellen. PhD Thesis, Be-richte aus der Mikro- und Feinwerktechnik, vol 17, Shaker Verlag, Aachen
30. Si-Mat (2015) Silicon materials. <http://si-mat.com/de/silizium-wafer.html>. Accessed 13 Aug 2015
31. Sugioka K, Cheng Y (2011) Integrated microchips for biological analysis fabricated by femtosecond laser direct writing. *MRS Bull* 36(12):1020–1027. doi:[10.1557/mrs.2011.274](https://doi.org/10.1557/mrs.2011.274)
32. Tiggelaar RM, Benito-López F, Hermes DC, Rathgen H, Egberink RJM, Mugele FG, Reinhoudt DN, van den Berg A, Verboom W, Gardeniers HJGE (2007) Fabrication, mechanical testing and application of high-pressure glass microreactor chips. *Chem Eng J* 131:163–170. doi:[10.1016/j.cej.2006.12.036](https://doi.org/10.1016/j.cej.2006.12.036)

33. Toepke MW, Beebe DJ (2006) PDMS absorption of small molecules and consequences in microfluidic applications. *Lab Chip* 6(12):1484–1486. doi:[10.1039/b612140c](https://doi.org/10.1039/b612140c)
34. Wikipedia (2015) Borosilicate glass. [http://www.wikipedia.org/wiki/Borosilicate\\_glass](http://www.wikipedia.org/wiki/Borosilicate_glass). Accessed 3 Aug 2015
35. Xia Y, Whitesides GM (1998) Soft lithography. *Annu Rev Mater Sci* 28:153–184
36. Xie L, Kirchberg S, Steuernagel L, Ziegmann G (2010) A mechanism influencing micro injection molded weld lines of hybrid nano filled polypropylene. *Microsyst Technol* 16(11):1855–1859

Microsystems for Pharmatechnology

Manipulation of Fluids, Particles, Droplets, and Cells

TU Braunschweig (Ed.)

2016, XI, 348 p. 154 illus., 95 illus. in color., Hardcover

ISBN: 978-3-319-26918-4